Asymmetry in the Indian Summer Monsoon Rainfall response to two types of La Niña evolution

Satyaban B. Ratna[1]*, Tanu Sharma[1], Arti Bandgar[1], O. P. Sreejith[1], D. S. Pai[2], M. Rajeevan[3], K. S. Hosalikar[1] and M. Mohapatra[4]

[1] Climate Research and Services, India Meteorological Department, Pune, India

[2] The Institute for Climate Change Studies (ICCS), Kottayam, Kerala, India

[3] National Centre for Earth Science Studies, Thiruvananthapuram, Kerala, India

[4] India Meteorological Department, New Delhi, India

*Correspondence to:
Satyaban B. Ratna
E-Mail: satyaban.ratna@imd.gov.in

ORCID
Satyaban B. Ratna https://orcid.org/0000-0001-8780-8165
Tanu Sharma https://orcid.org/0000-0002-2963-7174
Arti Bandgar
O. P. Sreejith https://orcid.org/0000-0002-3928-056X
D. S. Pai https://orcid.org/0000-0001-8392-5735
M. Rajeevan https://orcid.org/0000-0002-3000-2459
K. S. Hosalikar https://orcid.org/0009-0003-8941-3097
M. Mohapatra

Key Points:

- Two types of La Niña are distinguished for the June-September season based on whether they evolved from El Niño or La Niña in boreal winter.
- India receives more (less) summer monsoon rainfall when La Niña evolves from the El Niño (La Niña) in the previous boreal winter season.
- The difference in rainfall is linked to changes in large-scale atmospheric circulation over the tropical Indian and Pacific Oceans.

35   **Abstract**

36   This study attempts to understand the asymmetry in the Indian Summer Monsoon Rainfall (ISMR)

37   response to two types of La Niña whether they evolved from El Niño or La Niña in the previous

38   boreal winter season. It was seen that nine La Niña years during the monsoon season were preceded

39   by El Niño (hereafter ELLA) whereas eight were preceded by La Niña (hereafter LALA) during

40   the period 1961-2021. India received more rainfall during the ELLA years as compared to the

41   LALA years, linked to the difference in the Sea Surface Temperature (SST) and large-scale

42   atmospheric circulation anomalies over the tropical Pacific and Indian oceans. Based on the

43   strength and patterns of the cold SST anomaly and shift in the Walker circulation over the

44   equatorial Pacific Ocean, the enhanced (weakened) convection over the Indian landmass during

45   the ELLA (LALA) years, contributed to more (less) rainfall over India.

46

47   **Plain language summary**

48   A well-established inverse relationship between the El Niño-Southern Oscillation (ENSO) in the

49   equatorial Pacific Ocean and the Indian Summer Monsoon Rainfall (ISMR) is known but their

50   relationship is not always linear. It is also known that the evolution of La Niña events is not always

51   the same and hence their effect on the ISMR. Two types of La Niña events during the boreal

52   summer monsoon season are identified with respect to their evolution, whether there was an El

53   Niño or a La Niña during the previous boreal winter season, and they are termed ELLA and LALA

54   events, respectively. India receives higher ISMR during the ELLA years compared to the LALA

55   years due to the patterns and strength of SST anomaly and associated large-scale atmospheric

56   circulation over the tropical Pacific and Indian Oceans. The low-level convergence and enhanced

57   convection over the Indian landmass during ELLA years contribute to higher rainfall over India.

58   However, the low-level convergence and convection weakens over Indian region during LALA

59   years, reduces the rainfall over India. This study will be helpful for understanding the rainfall

60   variability over India based on the evolution of the SST anomaly in the equatorial Pacific Ocean.

63

1. Introduction

The Indian Summer Monsoon Rainfall (ISMR) or south-west monsoon from June to September (JJAS) season, is a land-atmosphere-ocean coupled system that contributes about 70 % of the annual rainfall over the Indian landmass (Shukla and Haung, 2016). The ISMR plays a crucial role in the agricultural and socio-economical structure of the subcontinent (Gadgil and Gadgil, 2006). The ISMR has a large range of temporal (from diurnal to multi-decadal) and spatial variability, which makes its prediction a challenge (Goswami, 2004). Many studies found that interannual variation of ISMR is linked to the changing boundary conditions at the local level as well as the remote teleconnections such as the Indian Ocean Dipole (IOD), Equatorial Indian Ocean Oscillation (EQUINOO), North Atlantic Oscillation (NAO), Pacific Decadal Oscillation (PDO), snow cover over Eurasia, Meridional Surface Air Temperature Anomaly Gradient Index (MTAGI) across Eurasia and El Niño Southern Oscillation (ENSO) (Kumar et al., 1999; Saji et al., 1999; Gillett et al., 2003; Pai, 2004; Gadgil et al., 2007; Hrudya et al., 2021; Ratna et al., 2021).

The ENSO is an ocean-atmospheric coupled phenomenon having a quasi-periodic nature. The typical life cycle of ENSO consists of its growth in boreal spring or summer, reaching its peak in winter, and decay in the following spring (Jin et al., 1994; Tziperman et al., 1994; Iwakiri and Watanabe, 2021). The ENSO is the most prominent forcing on the ISMR which explains almost 29% of its total interannual variability (Chakraborty and Singhai, 2021). The ISMR shows a negative correlation with the simultaneous central-equatorial Pacific (Niño 3.4 region: area over 5 °S-5 °N and 170 °W-120 °W) sea surface temperature (SST) anomalies. As a result of that, the La Niña (El Niño) event enhances (weakens) the ISMR through the displacement of the Walker circulation (Sikka and Gadgil, 1980; Webster and Yang, 1992; Kirtman and Shukla, 2000). However, every monsoon drought and flood is not associated with the ENSO condition (Roxy and Chaithra, 2018).

The oscillatory behavior of ENSO is inconsistent with respect to its temporal evolution and the transition among its phases such as El Niño, La Niña, and Neutral (Neelin et al., 2000; Timmermann et al., 2018). According to the study by Dommenget et al (2013), all the El Niño and La Niña events are not the same as there is a non-linearity in the amplitude, spatial pattern, and time evolution of these events. A study by Cole (2002) discussed that generally, the El Niño phase ends quickly whereas the La Niña phase lasts longer (multi-year La Niña). It is found in

94 observations that after a strong El Niño, the probability of occurrence of a multi-year La Niña is
95 high and this multi-year La Niña events are occurring more frequently in recent decades
96 (Dommenget et al., 2013).

97 As every ENSO event is not the same in terms of evolution, spread and intensity; its impact on the
98 ISMR is asymmetric. This made us curious to study how the different evolutions of the cold phase
99 of the ENSO (La Niña) influence the ISMR differently. We identified two types of La Niña events,
100 where the La Niña events are preceded by El Niño (ELLA) in the previous boreal winter and the
101 other one is La Niña preceded by La Niña (LALA) in the previous boreal winter; during the period
102 1961-2021. The objective of this study is (i) to understand the changes in the SST and the spatial
103 pattern of rainfall over India with respect to these two types of La Niña events (ELLA and LALA);
104 (ii) to understand the dynamics in terms of large-scale circulation patterns for two types of La Niña
105 that contributes to rainfall anomalies over India. The paper is organized as follows: Section 2
106 describes the data and the methodology applied for this study. Section 3 is dedicated to the results
107 and discussions; section 4 summarizes the findings of the work.

108

109 **2. Data and Methodology**

110 **2.1 Data**

111 The Oceanic Niño Index (ONI) from 1961 to 2021, is taken from the National Weather Service
112 website *https://origin.cpc.ncep.noaa.gov/products/analysis_monitoring/ensostuff/ONI_v5.php*
113 NOAA. ONI is one of the primary indicators for the oceanic component of the ENSO (3-month
114 running mean of ERSST.v5 SST anomalies in the Niño 3.4 region), based on a centered 30-year
115 base period. The rainfall dataset used for the study is the high spatial resolution (0.25 ° x 0.25 °)
116 gridded monthly data for the Indian region, for the period 1901-2021, prepared by the India
117 Meteorological Department (Pai et al., 2014). For SST, the NOAA Extended Reconstructed Sea
118 monthly Surface Temperature (ERSST) dataset (Huang et al., 2017) downloaded from the website
119 *https://psl.noaa.gov* which is available from January 1854 continuing to the present. For the
120 horizontal wind velocity components (u and v) and vertical wind velocity (omega), we used
121 monthly mean NCEP-NCAR Reanalysis 1 data (Kalnay et al., 1996) provided by the NOAA PSL,
122 Boulder, Colorado, USA, from their website at *https://psl.noaa.gov* for the period January 1948 to
123 April 2022.

2.2 Methodology

Defining ELLA and LALA events:

During the JJAS season, we considered those years as La Niña, for which the 3-month running mean of SST anomaly over the Niño 3.4 region (5 °N - 5 °S and 120 °W - 170 °W) is less than or equal to -0.5 °C during June-July-August (JJA) and July-August-September (JAS) seasons. Similarly, during the previous boreal winter, December-January-February (DJF) season, we considered those years as La Niña (El Niño), during which the 3-month mean Niño 3.4 region is less (more) than -0.5 °C (0.5 °C). Based on the time evolution of ONI, we categorize two types of La Niña events: 1). La Niña in the JJAS season is preceded by El Niño in the DJF season, as 'ELLA'. 2). La Niña in the JJAS season is preceded by La Niña in the DJF season, as 'LALA'. From 1961 to 2021, as per the above criteria, we found 17 years in which the La Niña event occurred during the JJAS season. Out of these 17 La Niña, 9 are identified as ELLA and 8 as LALA years. The list of ELLA years are 1964, 1970, 1973, 1988, 1998, 2007, 2010, 2016, and 2020.; and the list of LALA years are 1971, 1974, 1975, 1985, 1999, 2000, 2011, and 2021.

In order to understand how the two types of La Niña (ELLA and LALA) influence the ISMR, the composite analysis of rainfall, SST and winds are analyzed. All the anomalies are calculated with respect to the 1961-2020 climatology. We detrended the SST anomalies to remove the influence of basin-wide warming because of climate change. To understand the dynamical response of ELLA and LALA on ISMR, we examined the Walker circulations using zonal (u) components of the wind and the vertical velocity (ω), the velocity potential is also analyzed. The statistical significance of the composite anomalies is carried out with Student's t-test method.

3. Results and Discussion

3.1 Comparison of SST anomaly for ELLA and LALA events

The SST anomalies over the Indo-Pacific region play an important role in modulating spatial and temporal variability of the monsoon (Krishna Kumar et al., 2023; Cherchi et al., 2021). Figure 1(a) shows the time evolution of the ONI during the 3-month seasons for all the ELLA and LALA years. The figure shows the evolution of 17 La Niña years in which there are 9 ELLA years and 8 LALA years. The mean ONI values for ELLA (red) and LALA (blue) years are clearly showing the evolution of two types of La Niña events (Fig. 1a). It is clearly indicating that ELLA (LALA) events are evolving from a warm (cold) phase of ENSO in the boreal winter to La Niña in the

154 summer monsoon (JJAS) season (Fig. 1a, b). It was also observed that there is a difference in the
155 mean intensity of ONI value for the JJAS season during the ELLA and LALA years. The mean
156 intensity of La Niña during the summer monsoon season is higher for ELLA years as compared to
157 LALA years. (Fig. 1a). To understand the evolution of ELLA and LALA events in detail, the
158 composites of the detrended SST anomalies were plotted over the tropical Indo-Pacific Ocean.
159 Figures 1(b) and 1(d) show the spatial pattern of the SST anomaly corresponding to ELLA during
160 the DJF and the JJAS season respectively. In ELLA during the DJF season (Fig. 1b), positive and
161 statistically significant SST anomalies are seen over the eastern Pacific Ocean, extending up to the
162 central Pacific. The western Pacific Ocean is found to be relatively cold and positive SST
163 anomalies are observed over the Indian Ocean. During the JJAS season (Fig. 1d), a clear cold
164 tongue signature pattern of La Niña is seen with significant negative SST anomalies extended from
165 the eastern coast up to the central Pacific Ocean. Significant positive SST anomalies are visible
166 over the north Indian Ocean and the Maritime continent region. In terms of LALA composite
167 during the DJF season (Fig. 1c) statistically significant cold SST anomalies are seen over the
168 eastern Pacific Ocean, extending up to the central Pacific. The western Pacific Ocean is found to
169 be relatively warmer. However, negative SST anomalies are observed over the north Indian Ocean.
170 In the LALA composite during the JJAS season (Fig. 1e), a large spread of the significantly
171 negative SST anomaly is seen over the eastern and central Pacific Ocean. At the same time,
172 negative SST anomalies are present over the Indian Ocean. The comparison of SST anomalies
173 between two types of La Niña during the JJAS season indicates that the spread of cold SST
174 anomaly over the equatorial Pacific is narrow and strong during the ELLA composite whereas the
175 spread of cold SST anomaly over the equatorial Pacific is relatively weak and wider in the LALA
176 composite (Fig. 1d,e). The noticeable difference between the two composites also over the Indian
177 Ocean indicates a warm SST anomaly observed over the north Indian Ocean during ELLA years
178 whereas a cold SST anomaly is observed during LALA years. It is interesting to see whether such
179 differences in SST anomalies over the Indo-Pacific Ocean during ELLA and LALA years have an
180 influence on the ISMR variability which is analyzed in the next section.
181

182 **3.2 Comparison of rainfall over India for ELLA and LALA events**
183 We analyzed the composites of percentage rainfall anomaly patterns during the JJAS season over
184 the Indian region corresponding to the ELLA and LALA years (Fig. 2a and 2b). We found that

185 during ELLA (Fig. 2a), the ISMR is characterized by significant positive rainfall anomalies over

186 peninsular India, west-central India, north-western India, and some parts of north-eastern India.

187 Negative percentage rainfall anomalies are found over parts of the Indo-Gangetic plains. On the

188 contrary, the LALA composite (Fig. 2b) is characterized by a significantly negative percentage

189 rainfall anomaly over northern parts of peninsular India, southern parts of central India, and parts

190 of western India, especially near the Gujarat region. Positive percentage rainfall anomaly values

191 are found over the north-central and Indo-Gangetic plains. This spatial distribution of rainfall

192 anomaly indicates that India receives above-normal rainfall over many regions of the country

193 during ELLA years, as compared to LALA years (Fig. 2a and b). It was also seen that India as a

194 whole on average received about 9% above normal rainfall during ELLA composite years

195 compared to only about 1% above normal rainfall during the LALA composite, as per the India

196 Meteorological Department (IMD) observed ISMR data. It was also interesting to note that the

197 western parts of India (Indo-Gangetic plains) receive above (below) normal rainfall during ELLA

198 (LALA) years (Fig. 2a and b). It is now interesting to see the circulation patterns that controls the

199 asymmetry in the rainfall behaviors over India during ELLA and LALA years.

200

201 **3.3 Large-scale circulation over the Indo-Pacific region**

202 We have examined the composite of moisture divergence and transport at 850 hPa during the JJAS

203 season over Indian regions for ELLA and LALA years and presented in Fig 2c and 2d. The low-

204 level westerly winds over the warm Arabian Sea and the north Indian Ocean is conducive to bring

205 moist air from the Indian Ocean to the Indian landmass contributes to rainfall over India((Behera

206 and Ratnam, 2018; Ratna et al. 2015). As seen in Figure 2c, for the ELLA composite, the south-

207 westerly flow of the moisture flux transport is clearly visible, taking moisture supply to the western

208 parts of India; which causes the moisture convergence and hence positive values of the percentage

209 rainfall anomaly over these areas (Fig. 2a). However, during the LALA composite (Fig. 2d), the

210 south-westerly moisture supply to India is reduced compared to the ELLA composite and there is

211 zone of moisture divergence over western parts India contributing to below normal rainfall. At

212 the same time, a significant value of moisture flux convergence over the Indo-Gangetic plains

213 contributed to the above-normal rainfall during the LALA years (Fig. 2b).

214

To understand the mechanism and large-scale circulation responsible for the asymmetry in the rainfall pattern over India for ELLA and LALA composites during the monsoon season, we analyzed the velocity potential (shaded) along with the divergent wind (vector) at the upper-level (200 hPa) of the atmosphere in figure 3a and figure 3b. In the ELLA composite (Fig. 3a), strong convergent of wind vectors and positive values of the velocity potential anomaly are seen over the central Pacific Ocean. The upper-level divergent wind vectors and negative velocity potential anomaly are present over the Maritime continent, the Indian Ocean, and the Indian landmass associated with warm SST anomaly over the region (Fig. 2d). This indicates a low-level convergence and strong convection that represents in terms of rainfall anomaly over India in the ELLA composite (Fig. 2a).In the case of LALA composite (Fig. 3b), the converging wind vector and positive values of the velocity potential anomaly are still present over the central Pacific region but the magnitude, as well as the spread of these values, is reduced compared to the ELLA composite. At the same time, the divergent wind vector gets shifted southeastward and shows relatively weak negative values of the velocity potential over the western Pacific Ocean and Australia. This indicates that the upper-level divergence over the Indian landmass is reduced during LALA years and represents the weakening of low-level convergence over Indian landmass during LALA years compared to the ELLA years. This is coinciding well with the Indian landmass receiving less rainfall during LALA years compared to ELLA years (Fig. 2a and b).

Many observational studies show that the pressure oscillations and winds over the Indo-Pacific region can modulate the ISMR pattern up to a large extent (Walker, 1918; Ropelewski and Halpert, 1987; Hrudya, 2021, Ratna et al., 2021). To understand the ascending and descending motion over the tropical Indo-Pacific region and its contribution to the ISMR during ELLA and LALA composites; we analyzed the large-scale east-west tropical Walker circulation features over the Indo-Pacific region (Fig. 3c and Fig 3d). It was seen in the ELLA composite (Fig. 3c), a strong descending motion can be seen over the eastern and central Pacific Ocean whereas an ascending motion is seen over the Indian landmass and tropical Indian Ocean region (60 ⁰E to 90 ⁰E), a typical La Niña pattern. This ascending motion over the Indian region represents low-level convergence and enhanced convection contributes to more rainfall over India. However, this ascending motion over the Indian Ocean gets shifted eastward (near 120 ⁰E) in the LALA composite (Fig. 3d), coincides with the eastward shift seen in the velocity potential and divergent winds (Fig. 3a and

246 Fig. 3b). This indicates that the low-level convergence and the rising motion over the Indian
247 landmass region weakens and shifts southeastward reducing the convection and hence reducing
248 the intensity of rainfall over India during LALA events.
249
250 **4. Conclusion**
251 In the present study, we examined the response of the Indian summer monsoon rainfall with respect
252 to the two types of La Niña evolution by analyzing the composites of the SST, rainfall, the
253 atmospheric circulation features using velocity potential, divergent wind anomalies, and the
254 Walker circulation. We categorized the cold phase of the ENSO (La Niña) into two types based
255 on the evolution of Niño 3.4 index in the Pacific Ocean. The La Niña condition in the summer
256 monsoon (JJAS) season preceded by the El Niño (La Niña) condition in the previous boreal winter
257 (DJF) season is termed ELLA (LALA). Based on the two types of La Niña evolution, we identified
258 nine ELLA and eight LALA events during the period 1961-2021.
259
260 It was found that India received above-normal rainfall during the ELLA years compared to the
261 LALA years. Spatial distribution of the rainfall anomaly for the JJAS season showed a significant
262 positive value over most parts of India including peninsular India, central-western India, north-
263 western India, and some parts of north-eastern India during ELLA years. Whereas during LALA,
264 positive rainfall anomaly values are found only over the north-central and Indo-Gangetic plains.
265 At the same time a significant negative percentage rainfall anomaly was present over western
266 India, especially near the Gujarat region as well as northern parts of peninsula India. The
267 comparison between the two rainfall composites indicated a significant reduction in the ISMR over
268 the major parts of India during the LALA years compared to the ELLA years.
269
270 It was observed during the JJAS season that significant negative SST anomalies are present over
271 the eastern and central Pacific Ocean for the ELLA events. Whereas significant positive SST
272 anomalies in the western Pacific Ocean and the neighborhood of the Maritime continent. However,
273 significant negative SST anomalies were present mostly over the central Pacific Ocean but with a
274 weaker intensity during LALA events. This clearly indicated that SST anomalies over the tropical
275 Indo-Pacific Ocean are different in terms of distribution and intensity for the ELLA and LALA
276 years.

277 The dynamical analysis during the ELLA composite indicates a well-established moisture flux
278 transport at the lower level (850 hPa) from the warm Arabian Sea towards India and causing
279 moisture convergence over western parts of India. This moisture convergence over the western
280 India region is contributing to the above-normal rainfall. However, during LALA, the moisture
281 transport from cold Arabian Sea was reduced towards India, and a zone of significant moisture
282 flux divergence was observed over western India, thereby contributing to the negative rainfall
283 anomaly over central-western India. Further analysis of large-scale circulation indicates, an upper-
284 level divergence represents a low-level convergence and enhanced convection over the Indian
285 landmass contributing to above normal rainfall during ELLA years. In the case of LALA, the weak
286 or absence of upper-level divergence over Indian landmass indicates the weakening of low-level
287 convergence over the Indian landmass and hence the reduction of the ISMR.

288

289 In conclusion, the low-level convergence and enhanced rising motion over the Indian landmass
290 contribute to the enhanced convection and the above-normal rainfall over India during ELLA
291 years. However, the low-level convergence and the rising motion over the Indian region weakens
292 and shifts southeastward, reducing the convection and hence reducing the intensity of rainfall over
293 India during LALA years. Many earlier studies showed a well-established inverse relationship
294 between the La Niña and the ISMR (Sikka and Gadgil, 1980; Webster and Yang, 1992; Samanta
295 et al., 2020; Sharma et al., 2023). However, the present study concluded how different types of La
296 Niña evolution contributed to the difference in the rainfall distribution for the Indian summer
297 monsoon by modulating the large-scale atmospheric circulation and the monsoon winds over the
298 tropical Indo-Pacific Ocean. This study will be helpful for better understanding of the distribution
299 and intensity of rainfall anomaly over India based on the evolution of the SST anomaly in the
300 equatorial Pacific Ocean.

301

Conflict of Interest

The authors declare no conflicts of interest relevant to this study.

Open Research

The data used in this study can be downloaded from the following websites: Oceanic Niño Index (ONI) data available at https://origin.cpc.ncep.noaa.gov/products/analysis_monitoring/ensostuff/ONI_v5.php; rainfall data prepared by the India Meteorological Department (Pai et al., 2014) available at https://www.imdpune.gov.in/cmpg/Griddata/Rainfall_25_NetCDF.html; Extended Reconstructed Sea monthly Surface Temperature (ERSST, Huang et al., 2017) available at https://psl.noaa.gov/data/gridded/data.noaa.ersst.v5.html; horizontal wind velocity components (u, v) and vertical wind velocity (w) are used from NCEP-NCAR Reanalysis 1 (Kalnay et al., 1996) available at https://psl.noaa.gov/data/gridded/data.ncep.reanalysis.html

References

Behera, S. K., & Ratnam, J. V. (2018). Quasi-asymmetric response of the Indian summer monsoon rainfall to opposite phases of the IOD. Scientific Reports, 8, 123. https://doi.org/10.1038/s41598-017-18396-6

Chakraborty, A., & Singhai, P. (2021). Asymmetric response of the Indian summer monsoon to positive and negative phases of major tropical climate patterns. *Nature Scientific Reports*, 11:22561, 1-13. https://doi.org/10.1038/s41598-021-01758-6

Cole, J. E. (2002). Multiyear La Niña events and persistent drought in the contiguous United States. *Geophysical Research Letters*, 29, 1-4. https://doi.org/10.1029/2001GL013561

Cherchi, A., Terray, P., Ratna, S. B., Sankar, S., Sooraj, K. P., and Behera, S. (2021). Chapter 8 - Indian Ocean Dipole influence on Indian summer monsoon and ENSO: A review, Indian Summer Monsoon Variability. *Elsevier*, ISBN 9780128224021, 157-182. https://doi.org/10.1016/B978-0-12-822402-1.00011-9

Collins, M., An, S. I., & Cai, W. e. a. (2010). The impact of global warming on the tropical Pacific Ocean and El Niño. *Nature Geoscience*, 3, 391–397. https://doi.org/10.1038/ngeo868

Dommenget, D., Bayr, T., & Frauen, C. (2013). Analysis of the non-linearity in the pattern and time evolution of El Niño southern oscillation. *Climate Dynamics*, 40, 2825–2847. https://doi.org/10.1007/s00382-012-1475-0

Gadgil, S., & Gadgil, S. (2006). The Indian monsoon, GDP and agriculture. *Economic and Political Weekly*, 41, 4887–4895.

Gadgil, S., Rajeevan M. and Francis P. A. (2007). Monsoon variability: links to major oscillations over the equatorial Pacific and Indian oceans. *Current Science,* 93, 182–94.

361   Gillett, N. P., Graf, H. F., & Osborn, T. J. (2003). Climate change and the North Atlantic

362   oscillation. *Geophysical Monograph American Geophysical Union*, 134, 193–210.

363   https://doi.org/10.1029/134GM09

364   Goswami, B. N. (2004). South Asian Summer Monsoon: An Overview; in the Global Monsoon

365   System: Research and Forecast [Third International Workshop on Monsoon (IWM-III) (WMO

366   TD 1266) (2-6 November)].

367   http://www.wmo.int/pages/prog/arep/tmrp/documentd/global_monsoon_system_IWM3.pdf.

368   Hrudya, P. H., Varikoden, H., & Vishnu, R. (2021). A review on the Indian summer monsoon

369   rainfall, variability and its association with ENSO and IOD. *Meteorology and Atmospheric*

370   *Physics*, 133, 1-14. https://doi.org/10.1007/s00703-020-00734-5

371   Huang, B., & Peter, W. et. al. (2017). Extended Reconstructed Sea Surface Temperature version

372   5 (ERSSTv5), Upgrades, validations, and intercomparisons. *Journal of Climate*, 30, 8179-8205.

373   https://doi.org/10.1175/JCLI-D-16-0836.1

374   Iwakiri, T., & Watanabe, M. (2021). Mechanisms linking multi-year La Niña with preceding

375   strong El Niño. *Scientific Reports,* 11, 17465. https://doi.org/10.1038/s41598-021-96056-6

376   Jin, F. F., Neelin, J. D., & Ghil, M. E. (1994). El Niño on the devil's staircase: Annual

377   subharmonic steps to chaos. *Science, 264*, 70-72.

378   https://www.science.org/doi/10.1126/science.264.5155.70

379   Kalnay, E., Kanamitsu, M., Kistler, R., Collins, W., Deaven, D., Gandin, L., Iredell, M., Saha,

380   S., White, G., Woollen, J., & Zhu, Y. (1996). The NCEP/NCAR 40–issued reanalysis project.

381   *Bulletin of the American Meteorological Society*, 77, 437–472. https://doi.org/10.1175/1520-

382   0477(1996)077<0437:TNYRP>2.0.CO;2

383   Krishna Kumar, E. K., Abhilash, S., Syam, S., Vijaykumar, P., Santosh, K. R., & Sreenath, A. V.

384   (2023). Contrasting Regional Responses of Indian Summer Monsoon Rainfall to Exhausted

385   Spring and Concurrently Emerging Summer El Niño Events. *Advances in Atmospheric Sciences.*

386   https://doi.org/10.1007/s00376-022-2114-2

387   Kritman, B., & Shukla, J. (2000). Influence of the Indian summer monsoon on ENSO. *Quarterly*

388   *Journal of the Royal Meteorological Society*, 126, 213–239.

389   https://doi.org/10.1002/qj.49712656211

390   Kumar, K. K., Rajagopalan, B., & Cane, M. A. (1999). On the Weakening Relationship Between

391   the Indian Monsoon and ENSO. *Science*, 284(5423), 2156-2159.

392   https://www.science.org/doi/10.1126/science.284.5423.2156

393   Neelin, J. D., Jin, F. F., & Syu, H. H. (2000). Variations in ENSO phase locking. *Journal of*

394   *Climate*, 13, 2570–2590. https://doi.org/10.1175/1520-0442(2000)013<2570:VIEPL>2.0.CO;2

395   Pai, D. S. (2004). A possible mechanism for the weakening of El Nino-monsoon relationship

396   during the recent decades. *Meteorology and Atmospheric Physics*, 86, 143-157.

397   https://doi.org/10.1007/s00703-003-0608-8

398   Pai, D. S., Sridhar, L., Rajeevan, M., Sreejith, O. P., & Mukhopadhyay, B. (2014). Development

399   of a new high spatial resolution (0.25° X 0.25°) Long period (1901-2010) daily gridded rainfall

400   data set over India and its comparison with existing data sets over the region. *Mausam*, 65, 1-18.

401   https://doi.org/10.54302/mausam.v65i1.851

402   Rasmusson, E. M., & Carpenter, T. H. (1983). The Relationship Between Eastern Equatorial

403   Pacific Sea Surface Temperatures and Rainfall over India and Sri Lanka. *Monthly Weather*

404   *Review*, 111, 517-528. https://doi.org/10.1175/1520-0493(1983)111<0517:TRBEEP>2.0.CO;2

405   Ratna, S. B., Cherchi, A., Osborn, T. J., Joshi, M., & Uppara, U. (2021). The Extreme Positive

406   Indian Ocean Dipole of 2019 and Associated Indian Summer Monsoon Rainfall Response.

407   *Geophysical Research Letters*, 48, 1-11.   https://doi.org/10.1029/2020GL091497

408   Ratna, S.B., Cherchi, A., Joseph, P.V., Behera, S. K., Abish, B., Masina, S. (2015). Moisture

409   variability over the Indo-Pacific region and its influence on the Indian summer monsoon rainfall.

410   Climate Dynamics 46, 949–965. https://doi.org/10.1007/s00382-015-2624-z

411   Ropelewski, C. F., & Halpert, M. S. (1987). Global and Regional Scale Precipitation Patterns

412   Associated with the El Niño/Southern Oscillation. *Monthly Weather Review*, 115, 1606-1626.

413   https://doi.org/10.1175/1520-0493(1987)115<1606:GARSPP>2.0.CO;2

414   Roxy, M. K., & Chaithra, S. T. (2018). Climate Change and Water Resources in India.Chapter 2:

415   Impacts of Climate Change on the Indian Summer Monsoon. Ministry of Environment, Forest

416   and Climate Change (MoEF & CC), Government of India. ISBN: 978-81-933131-6-9

417   Saji, N. H., Goswami, B. N., Vinayachandran, P. N., & Yamagata, T. (1999). A dipole mode in

418   the tropical Indian Ocean. *Nature*, 401, 360-363. https://doi.org/10.1038/43854

419   Samanta, D., Rajagopalan, B., Karnauskas, K. B., Zhang, L., & Goodkin, N. F. (2020). La Niña's

420   diminishing fingerprint on the central Indian summer monsoon. Geophysical Research Letters,

421   47, e2019GL086237. https://doi.org/10.1029/2019GL086237

422   Sharma, T., Ratna, S. B., Pai, D. S. (2023). Modulation of Indian Summer Monsoon Rainfall

423   response to ENSO in the recent decades and its large-scale dynamics. PREPRINT (Version 1)

424   available at Research Square [https://doi.org/10.21203/rs.3.rs-2405719/v1]

425   Shukla, R. P., & Haung, B. (2016). Interannual variability of the Indian summer monsoon

426   associated with the air-sea feedback in the northern Indian Ocean. *Climate Dynamics*, 46, 1977–

427   1990. https://doi.org/10.1007/s00382-015-2687-x

428 Sikka, D. R., & Gadgil, S. (1980). On the maximum cloud zone and the ITCZ over Indian

429 longitudes during the southwest monsoon. *Monthly Weather Review*, 108, 1840-1853.

430 https://doi.org/10.1175/1520-0493(1980)108<1840:OTMCZA>2.0.CO;2

431 Timmermann, A., An, S. I., & Kug, J. S. e. a. (2018). El Niño–Southern Oscillation complexity.

432 *Nature*, 559, 535–545. https://doi.org/10.1038/s41586-018-0252-6

433 Tziperman, E., Stone, L., Cane, M. A., & Jarosh, H. E. (1994). El Nino chaos: Overlapping of

434 resonances between the seasonal cycle and the Pacific ocean-atmosphere oscillator. *Science*, *264*,

435 72-74. https://www.science.org/doi/10.1126/science.264.5155.72

436 Walker, G. T. (1918). Correlation in seasonal variation of weather. *Quarterly Journal of the*

437 *Royal Meteorological Society*, 44, 223-224.

438 Webster, P. J., & Yang, S. (1992). Monsoon and ENSO: Selectively interactive systems.

439 *Quarterly Journal of the Royal Meteorological Society*, 118(507), 877–926.

440 https://doi.org/10.1002/qj.49711850705

441 Zhang, R. H., Gao, C., & Feng, L. (2022). Recent ENSO evolution and its real-time prediction

442 challenges. *National Science Review*, 9. https://doi.org/10.1093/nsr/nwac052

443

444

445
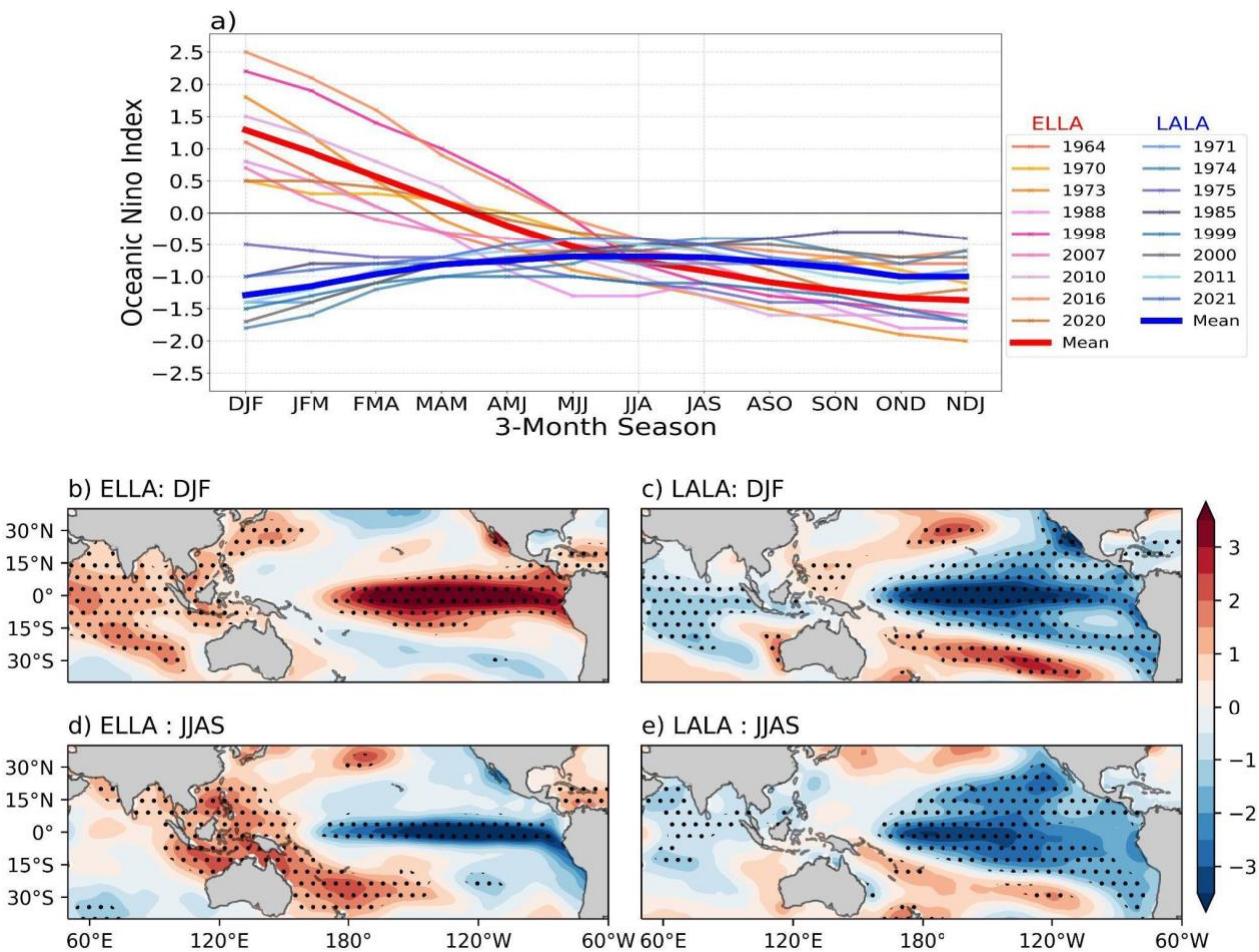
446

447

448

449

450

Figures:

Figure 1. a) Three-month season time series of Oceanic Niño Index (ONI) for ELLA (La Niña preceded by El Niño) and LALA (La Niña preceded by La Niña) years between 1961 to 2021. The mean ONI for ELLA and LALA years is represented by red and blue thick lines respectively. Detrended SST anomaly composites for **b)** ELLA (DJF) **d)** ELLA (JJAS) years. **c)** and **e)** are the same as b) and d) but for LALA years. Dotted marks (b – e) are significant values at the 90% confidence level based on the Student's t-test. For the anomaly calculation, 1961-2020 climatology is considered.
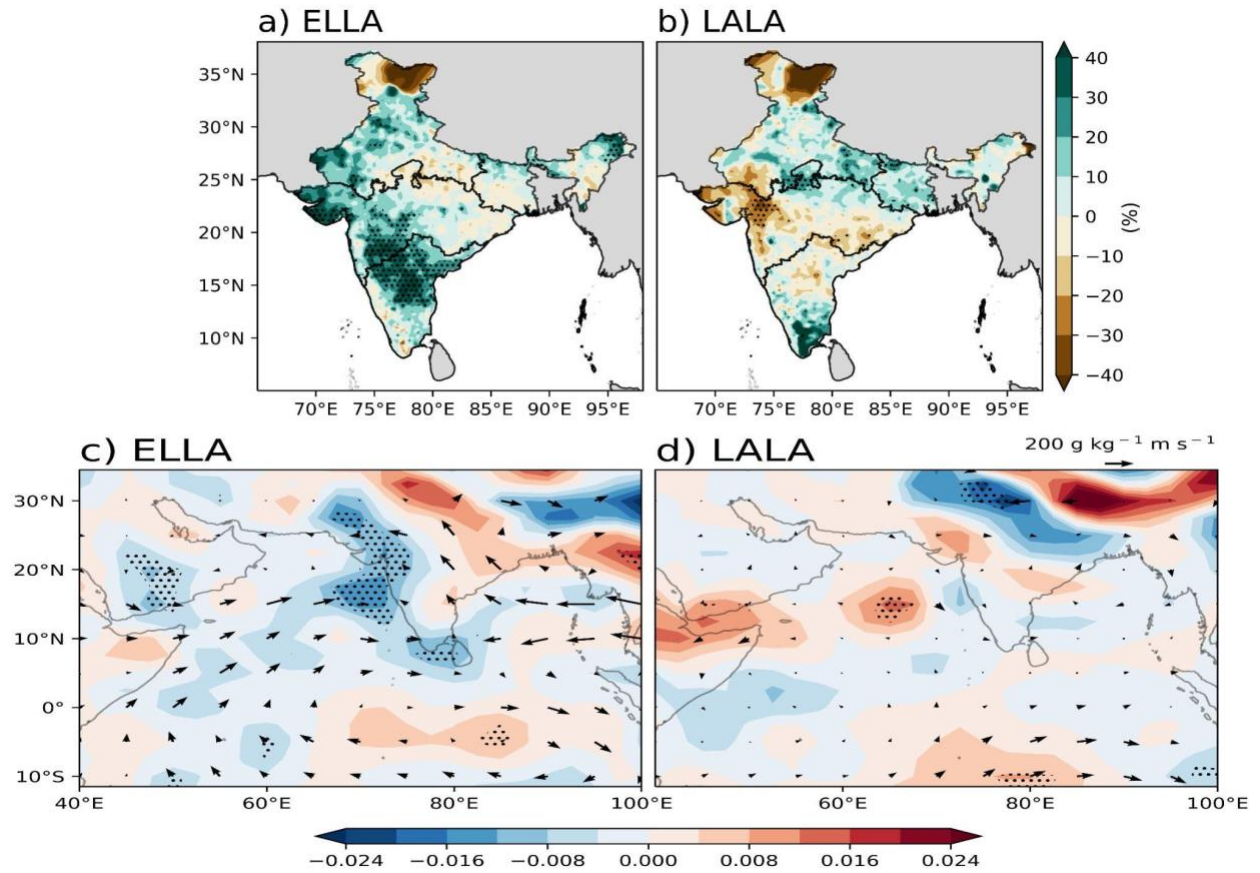
16

461

Figure 2. Percentage seasonal rainfall anomaly (June-September) composites for **a)** ELLA and **b)** LALA years. **c)** and **d)** are the same as a) and (b) but for moisture flux divergence (shaded, 10^2 s^{-1}) overlaid with moisture flux transport vector (g kg^{-1} m s^{-1}) at 850 hPa. Dotted marks are significant values at the 90% confidence level based on the Student's t-test. For the anomaly calculation, 1961-2020 climatology is considered.
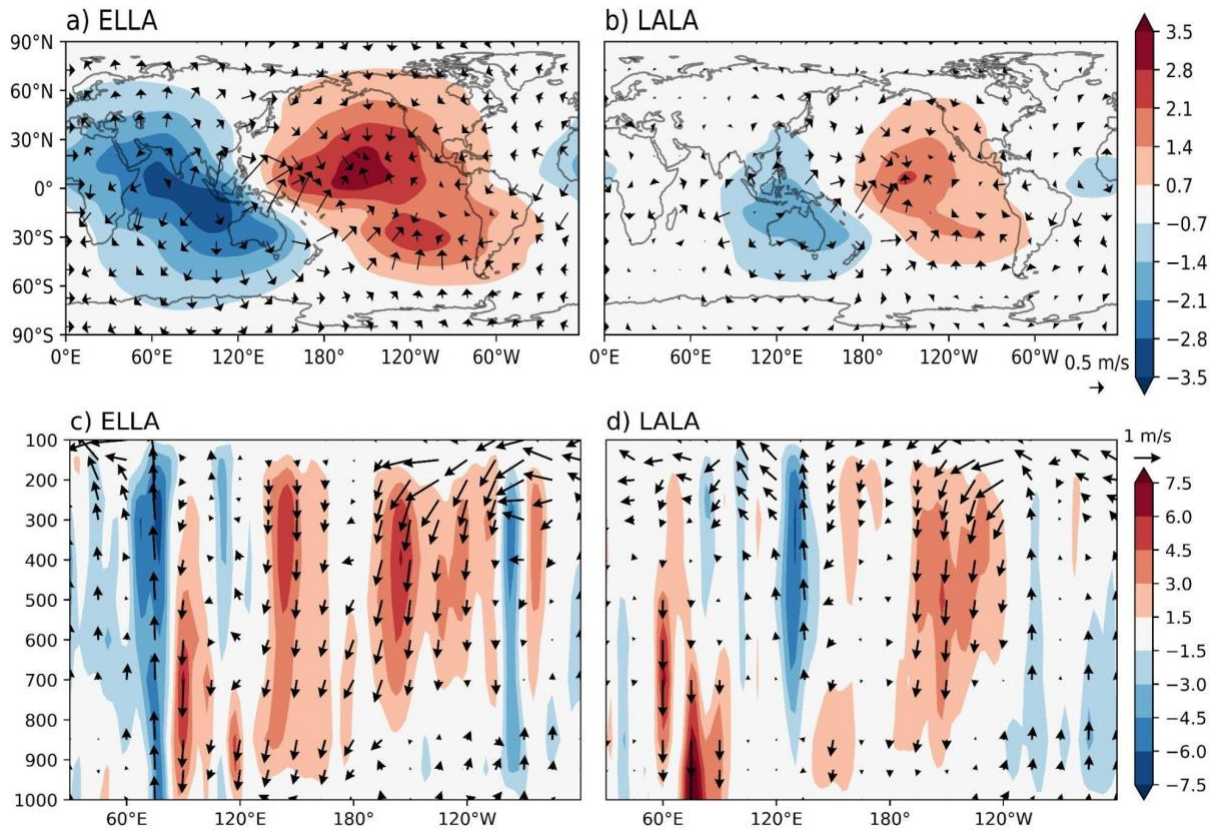
467

468

469

Figure 3. Velocity potential anomaly composite (shaded, $10^6 \times$ m² s⁻¹) along with the divergent wind (vector) at 200 hPa for **a)** ELLA and **b)** LALA years. Walker circulation anomalies over the Indo-Pacific sector for **c)** ELLA and **d)** LALA years. In c) and d) vector has zonal (u) and vertical (w) wind components, from 1000 hPa to 100 hPa pressure level and values are averaged over latitude 7.5 ⁰N - 37.5 ⁰N. Color contour representing w $\times$ 10³ m s⁻¹.

475

476

477

478

479

480